DECENTRALIZED VIBRATION CONTROL FOR ACTIVE HELICOPTER ROTOR BLADES

Dr. Peter Konstanzer
Mechtronics & Dynamics
EADS Corporate Research Centre
Munich, Germany

Abstract

Decentralized vibration control for active helicopter rotor blades is proposed to reduce rotor-induced vibration and to stabilize the rotor. The time-periodic behavior of the rotor is approximated by a time-invariant system in multiblade coordinates. Considering the rotor as an interconnection of N subsystems, the approximation is investigated in terms of subsystem interconnection errors. A new decentralized vibration control method is proposed which provides inherent robustness with respect to uncertain subsystem interconnections and thus, is appropriate to control the time-periodic system. The internal model principle is applied to achieve hubload compensation and hence a reduction of the rotor-induced vibration. Subsystem stabilizing controllers are applied for rotor stabilization. The control system is synthesized based on decentralized optimal output feedback. Several design examples for a BO105 helicopter rotor in forward flight demonstrate the performance of the method in achieving rotor-induced vibration reduction and rotor stabilization.

Nomenclature

$A, \mathcal{A}$	system matrix
$B, \mathcal{B}$	input matrix
$C, \mathcal{C}$	sensor matrix
D	feedthrough matrix
E	disturbance matrix
F	disturbance matrix, hub force
g	scalar feedback gain
H	Hamiltonian function
I	identity matrix
J	performance index
k	vector of feedback parameters
K	feedback gain matrix
M	hub moment
n	system order, index of harmonics
N	number of subsystems or blades
N_ψ	number of azimuth angles
Q	weighting matrix
r	relative degree
R	weighting matrix, rotor radius
T	transmissibility
u	input vector
w	disturbance vector, deflection
x	state vector, lagwise displacement
y	output vector
β	blade flapping angle
ζ	damping ratio
η	trailing edge flap deflection
λ	disturbance pole
σ	singular value
ψ	azimuth angle
ω	frequency
Ω	rotor frequency

0	collective form
$1c$	longitudinal cyclic form
$1s$	lateral cyclic form
$N/2$	differential form
β	out-of-plane flapping
c	compensation
ζ	in-plane lagging
m	rotor blade index
p	plant, pole
s	stabilization, sensor
z	zero

IBC	individual blade coordinate
LMS	lagging mode stabilization
LTI	linear time-invariant
LTP	linear time-periodic
MBC	multiblade coordinate
RDRC	robust disturbance rejection control
TEF	trailing edge flap

Introduction

Rotor-induced vibration in helicopters is the oscillatory response of the airframe due to periodically varying aerodynamic loads acting on the rotor blades. Due to these higher harmonic aerodynamic loads, the rotor blades execute a forced vibration and higher harmonic loads are generated at the blade roots. These loads are transmitted through the rotor hub to the nonrotating frame only at harmonics which are multiples of $N\Omega$ – the blade passage frequency. The transmitted hubloads in their part excite the airframe structure resulting in rotor-induced vibration at multiples of $N\Omega$. In steady flight, the rotor frequency Ω is known and deviations are small. Consequently, also the frequencies of the higher harmonic hubloads at multiples of $N\Omega$ are known. However, phase and amplitude of the hubloads are unknown and vary considerably with the flight condition.

In unsteady flight, the transient vibration response depends considerably on the damping of the system. Rotor stabilization is thus essential for active damping enhancement of the weakly damped in-plane lagging motion. Furthermore, rotor stabilization is important in order to prevent ground and air resonances.

Active rotor control, in the past only hardly feasible due to the lack of appropriate rotating blade actuation systems, is recently becoming feasible due to the availability of solid state actuators. This allows on-blade actuation even under high centrifugal and out-of-plane accelerations, e.g. to drive aerodynamic control surfaces on the blade. Particularly trailing edge flaps located at the outer part of the rotor blades seem to be suitable for reducing rotor-induced vibration as well as for rotor stabilization, see ENENKL at al. [12]. The higher harmonic loads acting on the blades can be complemented by additional loads generated by the deflection of the trailing edge flaps. Provided that the trailing edge flap deflections are properly controlled, this reduces the hub loads transmitted to the airframe and thus the rotor-induced vibration at the airframe. Rotor stabilization for active damping enhancement of the in-plane lagging motion may be achieved when the feedback principle is applied.

Feasibility studies of using active materials for rotor control motivated the development of actuation systems as proposed by BARRETT [2], BÜTER [3], CHOPRA et al. [7, 6, 33, 22], HAGOOD et al. [10], HALL et al. [37, 28, 29], SCHIMKE et al. [34], and STRAUB et al. [39, 40]. A focus has been put on trailing edge flaps and hover testing has been reported for some actuation systems, see CHOPRA et al. [20, 38], HALL et al. [14] and ROGERS et al. [31].

Regarding controller design, stabilization has been proposed for single rotor blades by HAM [16], KESSLER et al. [18], NITZSCHE [26], NARKIEWICZ [24], and considering time-periodic systems by WASIKOWSKI et al. [5], PANDIAN et al. [27], CALICO et al. [4]. Most of the investigations were however restricted to rigid blade motions. On the other hand, the conventional approach for reducing vibration at $N\Omega$ is based on a quasi-steady assumption, see SHAW et al. [35] and HALL et al. [15]. However, when the rotor-induced vibration problem is approached by dynamic feedback control to overcome the quasi-steady assumption, see ARCARA et al. [1], ROTTMAYR et al. [32], DIETERICH [11] and PRECHTL et al. [30], rotor stability will be affected. The vibration and stabilization problem can thus no longer be considered independently. Moreover, since rotor-induced vibration is due to the motion of the rotor as a whole, stabilization can no longer be designed by simply considering single blades.

The objective of this research is to develop an appropriate vibration control method for active helicopter rotor blades in order to achieve simultaneously rotor-induced vibration reduction and rotor stabilization. The resulting multivariable control system is required to possess a simple feedback structure which provides physical insight and may allow a certain degree of tuning during flight tests. The controller has further to deal with the time-periodic dynamical system behavior of a helicopter rotor in forward flight. Moreover, we seek for robustness of the control system with respect to uncertainties in the plant model, a variation of the flight speed regime, and small deviations of the rotor frequency Ω. Considering the rotor as an interconnection of N individual subsystems (rotor blades), a new vibration control method is proposed based on decentralized control, for details see KONSTANZER [19]. The proposed method will be investigated based on open-loop and closed-loop simulations of the time-periodic behavior of active helicopter rotor blades with on-blade actuation by trailing edge flaps.

System Analysis

For vibration control, the dynamic behavior of active helicopter rotor blades may be described by a linear time-periodic system. To simplify analysis, design and implementation of a multivariable control system, a representation by a linear time-invariant system is desired. However, any time-invariant representation of a time-periodic system can only be an approximation. A system analysis is presented and the applied constant coefficient approximation is discussed in terms of subsystem interconnection errors.

A single main rotor consisting of N identical rotor blades is considered in forward flight. The rotor is supposed to be fixed at the hub, thus neglecting the influence of the airframe. The blades are modeled as flexible beam structures, which perform a coupled motion consisting of out-of-plane flapping, in-plane lagging, and torsion. Trailing edge flaps [34] located at the outer part of the rotor blades are considered for aerodynamic on-blade actuation. The aeroservoelastic behavior is modeled using the comprehensive analytical model of rotorcraft aerodynamics and dynamics CAMRAD II [17].

Time-Periodic System

The dynamic behavior of active helicopter rotors may be described by a time-periodic dynamical system linearized about the periodic trim state. Linearization of the nonlinear time-periodic rotor system at N_ψ azimuth angles considering small perturbations in the flapping, lagging and torsional motion of the rotor blades as well as in the deflection of the trailing edge flaps leads to a linear time-periodic LTP system written in state-space representation as [17]

$$\dot{\tilde{x}} = \tilde{A}(\psi)\tilde{x} + \tilde{B}(\psi)\tilde{u} \quad (1)$$
$$\tilde{y} = \tilde{C}(\psi)\tilde{x} + \tilde{D}(\psi)\tilde{u} \quad (2)$$

The state vector $\tilde{x}$ consists of the structural degrees of freedom of the N individual rotor blades describing the flapping, lagging and torsional motion of the flexible blades. The control input $\tilde{u}$ corresponds to the trailing edge flap deflections and the output $\tilde{y}$ to individual blade sensor signals of the N rotor blades. The system matrices contain structural as well as aerodynamic terms resulting from a perturbed motion of the blades about the periodic trim state. Since the coefficients associated with the aerodynamic terms vary with the rotor revolution, the system matrices are periodic matrix functions of the reference azimuth angle ψ. The linear time-periodic system describes the aeroservoelastic behavior of the individual rotor blades in the rotating frame. System analysis and controller design may be performed in the rotating frame considering the dynamic behavior of the individual rotor blades.

Multiblade Coordinates

However, rotor-induced vibration is due to the motion of the rotor as a whole. This motivates the transformation into multiblade coordinates MBC which describe the motion of the rotor in the nonrotating frame [8].

The transformation is applied to the time-periodic system given by Eqs. (1, 2). This leads to a linear time-periodic system in multiblade coordinates

$$\dot{x} = A(\psi)x + B(\psi)u \quad (3)$$
$$y = C(\psi)x + D(\psi)u \quad (4)$$

where the state vector $x = [x_0, x_{1c}, x_{1s}, x_2]^T$ and the input vector $u = [u_0, u_{1c}, u_{1s}, u_2]^T$ are in multiblade coordinates consisting of collective, cyclic, and differential form.

Table 1: Plant models

	BO105 rotor fixed at hub (CAMRAD II)		
Regime	forward	descent	hover
TEF actuators	radial station	rel. length	rel. chord
	$0.6 \sim 0.7R$	$0.1R$	0.15
Hub load sensors	in-plane hub loads: $y_c = [F_x, F_y]^T$		
	out-of-plane hub loads: $y_c = [F_z, M_x, M_y]^T$		
On-blade sensors	lag displ. $y_s = [y_{\zeta 0}, y_{\zeta 1c}, y_{\zeta 1s}, y_{\zeta 2}]^T$		
	flap displ. $y_s = [y_{\beta 0}, y_{\beta 1c}, y_{\beta 1s}, y_{\beta 2}]^T$		
State variables	structural DOF consisting of 4 × flapping, 2 × lagging, 1 × tors. mode		
	system order	number of azimuth angles	
	$n = 56$	$N_\psi = 48$	

The output vector y contains hub load sensor outputs y_c and on-blade sensor outputs y_s again in multiblade coordinates. Details of the plant models investigated are given in Tab. 1.

Constant Coefficient Approximation

Controller design may be applied for the time-periodic system based on the Floquet-Lyapunov theory [4]. This may lead to periodic controller parameters depending on the flight condition. However, to simplify analysis, design and implementation, we are interested in the possibility of an accurate constant coefficient representation of the time-periodic system. For this purpose, the periodic matrix functions of the time-periodic system in multiblade coordinates are expanded in Fourier series, e.g. $A(\psi) = A + \sum_{k=1}^{\infty} A_{ck} \cos k\psi + A_{sk} \sin k\psi$, and by neglecting the periodic terms, a constant coefficient approximation is obtained in terms of a linear time-invariant

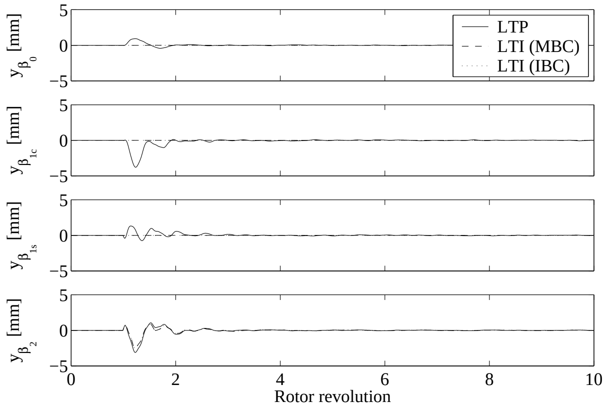

(a) Out-of-plane flapwise displacement

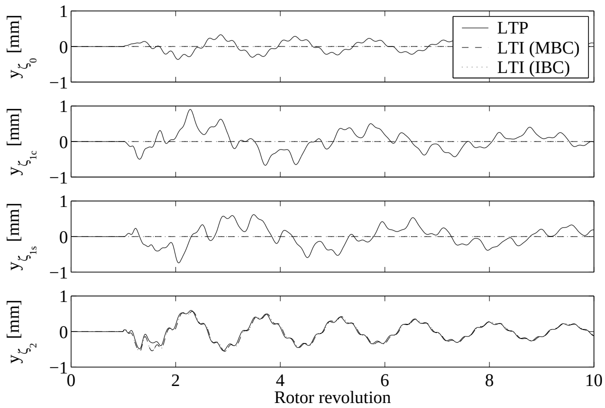

(b) In-plane lagwise displacement

Figure 1: Impulse response due to a differential input disturbance.

LTI system

$$\dot{x} = A\,x + B\,u \quad (5)$$
$$y = C\,x + D\,u \quad (6)$$

where the state vector $x = [x_0, x_{1c}, x_{1s}, x_2]^T$ consists of the structural degrees of freedom of the N flexible rotor blades in multiblade coordinates. The input vector $u = [u_0, u_{1c}, u_{1s}, u_2]^T$ consists of the trailing edge flap deflections in multiblade coordinates and the output vector y may contain hub load sensor outputs y_c as well as on-blade sensor outputs y_s again in multiblade coordinates. Representing the plant model by a constant coefficient approximation in multiblade coordinates allows analysis and controller design based on linear time-invariant systems, thus making the problem amenable to a wide range of multivariable controller design methods.

Interconnection Error

Any constant coefficient representation of a time-periodic system can only be an approximation. For a constant coefficient approximation in MBC, the interconnection of collective and cyclic forms is preserved whereas the interconnection of differential and non-differential forms is completely neglected leading to a considerable interconnection error, as shown by the impulse response given in Fig. 1. Here, the response due to an impulse disturbance applied at the differential input is observed through the out-of-plane flapwise and in-plane lagwise displacements in collective, cyclic and differential form. The constant coefficient approximations in individual blade coordinates LTI (IBC) and multiblade coordinates LTI (MBC) are compared to the correct time-periodic LTP system. For a differential impulse, the response of all non-differential forms is neglected. Whereas the interconnection of collective and cyclic forms is basically preserved, the interconnection of differential and non-differential forms is completely neglected by the constant coefficient approximation in multiblade coordinates. This is the interconnection error introduced by the constant coefficient approximation.

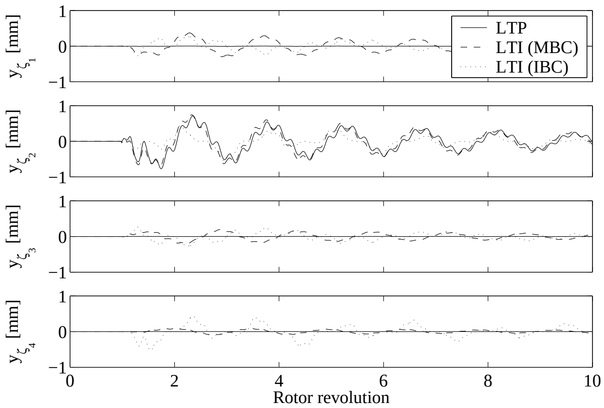

Figure 2: Impulse response for an input disturbance in IBC.

Neglecting interconnections between multiblade forms introduces false interconnections between the individual rotor blades. This is shown in Fig. 2 where the impulse response observed through the individual blades is given due to an input disturbance applied to one individual blade. Whereas the time-periodic system contains no interconnections between the individual blades, the constant coefficient approximations introduce an interconnection error between the individual blades.

Control System Synthesis

Considering the rotor as an interconnection of N individual subsystems (rotor blades), a new vibration control method is proposed based on decentralized control. The method accounts for the time-periodic system behavior of a helicopter rotor in forward flight by applying a decentralized feedback structure. To reduce rotor-induced vibration, robust disturbance rejection control is applied based on the internal model principle of feedback control. Rotor stabilization is addressed by individual subsystem (blade) stabilizing controllers constructed from dynamic compensators of known structure. To finally synthesize a decentralized vibration control system for active helicopter rotor blades, robust disturbance rejection and rotor stabilization are set into the framework of decentralized optimal output feedback.

In the control of active helicopter rotor blades, the decentralized control strategy [36] is particularly appropriate when individual rotating blade actuators and sensors are used.

Since helicopter rotors consist of N rotor blades, the application of decentralized subsystem controllers to each rotor blade seems to be a natural approach. Since all blades are identical, there is no reason for the subsystem controllers to be non-identical which introduces a considerable simplification into the control system.

However, when the motion of the rotor as a whole is considered in multiblade coordinates, the system becomes coupled. Decentralized control can provide inherent robustness with respect to the interconnection error introduced when the time-periodic system is approximated by a time-invariant system.

Decentralized Optimal Output Feedback

The static output feedback problem is to find a static output feedback matrix for a given linear time-invariant system, so that the closed-loop system has some desirable characteristics. Static output feedback will allow us to design controllers of any desired structure, e.g. fixed-order dynamic output feedback compensators or decentralized controllers.

Let the plant to be controlled be given by the following linear time-invariant system

$$\dot{x} = Ax + Bu \tag{7}$$

$$y = Cx \tag{8}$$

where $x(t) \in \mathbb{R}^n$ is the state vector, $u(t) \in \mathbb{R}^m$ the input vector, and $y(t) \in \mathbb{R}^p$ the vector of measured outputs. The feedback law is determined by the output feedbacks given by

$$u = Ky \tag{9}$$

where $K \in \mathbb{R}^{m \times p}$ is the matrix of constant/static feedback gains to be determined by the design procedure[1].

Static output feedback is important in its own, but also since many other problems can be reduced to it. Fixed-order dynamic compensation of order $q < n$ can be reduced to the static output feedback case [25]

In order to design decentralized controllers as well as dynamic compensators with prescribed structure using static output feedback, a feedback structure formulation allowing arbitrary output feedback structures is proposed.

[1] The case of non-strictly proper systems including feedthrough, i.e. $y = Cx + Du$ instead of Eqn. (8), may be put down to the strictly proper case by constructing a strictly proper auxiliary system simply by omitting the feedthrough. Suppose that a gain matrix $\tilde{K}$ has been determined for the auxiliary system. Then a comparison of the auxiliary system $\dot{x} = (A + B\tilde{K}C)x$ and the proper system $\dot{x} = (A + BK(I - DK)^{-1}C)x$ yields

$$\tilde{K} = K(I - DK)^{-1} \quad \text{or} \quad K = (I + \tilde{K}D)^{-1}\tilde{K} \tag{10}$$

where the gain matrix K for the non-strictly proper system is recovered from the gain matrix $\tilde{K}$ for the strictly proper auxiliary system.

Definition 1 *For the static output feedback law given by Eqn. (9), the arbitrary feedback structure formulation is defined as*

$$K \;=\; K_p + \sum_{i=1}^{m} t_i\, k^T\, U_i \qquad (11)$$

where $K_p \in \mathbb{R}^{m \times p}$ denotes the matrix of prescribed coefficients, $k \in \mathbb{R}^{v \times 1}$ the vector of v feedback parameters to be designed, and $t_i \in \mathbb{R}^{m \times 1}$ and $U_i \in \mathbb{R}^{v \times p}$ are vectors and matrices, respectively, which determine the entry of the feedback parameters k into the gain matrix K.

The linear quadratic regulator problem for decentralized optimal output feedback DOOF can be stated as follows, cp. [21]. Let the plant be given by Eqs. (7, 8) and the feedback law by Eqn. (9) and consider the arbitrary feedback structure formulation of Definition 1. Find a gain matrix K of arbitrarily specified structure that minimizes an infinite horizon quadratic performance index of the type

$$J \;=\; \frac{1}{2}\int_0^{\infty} (x^T\, Q\, x \,+\, u^T\, R\, u)\, dt \qquad (12)$$

where Q and R are symmetric positive semidefinite weighting matrices. The semidefiniteness assumptions on Q and R guarantee that J is non-negative and lead to a sensible minimization problem. The closed-loop system equations are

$$\dot{x} = (A + B\,(K_p + \sum_{i=1}^{m} t_i\, k^T\, U_i)\, C)\, x := A_{cl}\, x \qquad (13)$$

The dynamical optimization problem may be converted into an equivalent static problem. The symmetric matrix X is defined by $X = x(0)^T x(0)$. To solve the static problem the Lagrange multiplier approach [13] is applied which converts the constrained problem into an equivalent unconstrained problem by defining the Hamiltonian $H = \mathrm{tr}\,(MX) + \mathrm{tr}\,(FP)$ where P is a symmetric matrix of Lagrange multipliers to be determined. Setting the partial derivatives of H with respect to all independent variables M, P, k equal to zero yields the necessary conditions for the solution of the decentralized optimal output feedback problem given by the following theorem.

Theorem 1 *Let the plant be given by Eqs. (7, 8) and the feedback law by Eqn. (9) and consider the arbitrary feedback structure formulation of Definition 1. Then necessary conditions for the feedback gain K to minimize the performance index of Eqn. (12) subject to the closed-loop system constraint (13) are given by*

$$\begin{aligned}
0 &= X + A_{cl}P + P\,A_{cl}^T && (14)\\
0 &= A_{cl}^T M + M A_{cl} + Q + C^T K^T R K C && (15)\\
k &= -\left(\sum_{i,j=1}^{m} (t_i^T R\, t_j)\, U_i C P C^T U_j^T\right)^{-1} \\
&\quad \sum_{i=1}^{m} U_i C P\, (MB + C^T K_p^T R)\, t_i && (16)\\
K &= K_p + \sum_{i=1}^{m} t_i\, k^T U_i && (17)
\end{aligned}$$

Proof: see [19].

Robust Disturbance Rejection Control

In systems exposed to persistent external disturbances, a controller is required which regulates the effect of the external disturbances. In the rotor-induced vibration problem, rotor blades are exposed to persistent higher harmonic aerodynamic disturbances and the controller is required to regulate the effect at the rotor hub.

The internal model principle of control theory defines the necessary structure of a multivariable controller to achieve closed-loop stability and output regulation (e.g. disturbance rejection) in a system with deterministic disturbance and reference signals. Further, the controller is structurally stable or robust in the sense that output regulation occurs even in the presence of small perturbations of the system parameters.

Simply stated, a controller is structurally stable only if the controller uses feedback of the regulated variable, and incorporates in the feedback loop an internal model of the external signals (i.e. disturbance or reference signals) which the regulation is required to process.

Robust disturbance rejection control [9] applies the internal model principle. Let the plant to be controlled be given by the following linear time-invariant model

$$\begin{aligned}
\dot{x} &= Ax + Bu + Ew && (18)\\
y &= Cx + Du + Fw && (19)\\
y_m &= C_m x + D_m u + F_m w && (20)
\end{aligned}$$

where $x(t) \in \mathbb{R}^n$ is the state vector, $u(t) \in \mathbb{R}^m$ the input vector, $y(t) \in \mathbb{R}^r$ the vector of outputs to be regulated, $y_m(t) \in \mathbb{R}^{r_m}$ the vector of measurable outputs, and $w(t) \in \mathbb{R}^{m_d}$ the vector of disturbances. The class of disturbances acting on the plant are assumed to be given by the following system

$$\begin{aligned}
\dot{\eta} &= \mathcal{A}\eta && (21)\\
w &= \mathcal{C}\eta && (22)
\end{aligned}$$

The eigenvalues $\lambda_1(\mathcal{A}), \ldots, \lambda_p(\mathcal{A}) \in \mathbb{C}^+$ are called disturbance poles and characterize the type of the considered disturbance, e.g. constant, sinusoidal, triangular, polynomial-sinusoidal.

In the rotor-induced vibration problem, the uncontrolled hub loads are considered as disturbances w of sinusoidal type with frequency 4Ω and disturbance poles $\lambda_{1,2} = \pm j4\Omega$.

In robust disturbance rejection, one is interested in designing a controller so that the outputs y are independent of the external disturbances w, i.e. disturbance rejection is achieved. This leads to the requirement that the transmission of the disturbances w to the outputs y is zero in steady-state

$$\lim_{t\to\infty} y(t) \quad = \quad 0 \qquad \forall x(0), \eta(0) \tag{23}$$

Furthermore, the closed-loop system is required to be asymptotically stable and to possess robustness, i.e. disturbance rejection occurs for any perturbation in the plant model as long as the closed-loop system remains stable.

Any linear time-invariant controller that solves the robust disturbance rejection control problem is given by the feedback law

$$u \quad = \quad y_s + K_c x_c \tag{24}$$

which combines the output y_s of some stabilizing controller and the state x_c of the subsequently defined servo-compensator which is necessary to achieve robust disturbance rejection.

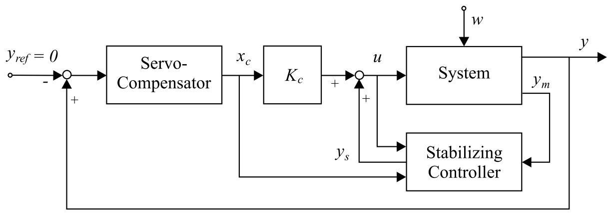

Figure 3: General robust disturbance rejection control.

Definition 2 (Servo-Compensator [9]) *The servo-compensator for the plant (18) – (20) is a dynamic compensator*

$$\dot{x}_c = A_c x_c + B_c y \tag{25}$$

with the inputs $y \in \mathbb{R}^r$ *and the outputs* $x_c \in \mathbb{R}^{n^*}$ $(n^* = rp)$ *given by*

$$A_c = \mathrm{blockdiag}\,\underbrace{(\hat{A}_c, \hat{A}_c, \ldots, \hat{A}_c)}_{r}$$
$$B_c = \mathrm{blockdiag}\,\underbrace{(\hat{B}_c, \hat{B}_c, \ldots, \hat{B}_c)}_{r} \tag{26}$$

$$\underset{p\times p}{\hat{A}_c} = \begin{bmatrix} 0 & 1 & 0 & \cdots & 0 \\ 0 & 0 & 1 & \cdots & 0 \\ \vdots & \vdots & \vdots & & \vdots \\ -\delta_1 & -\delta_2 & -\delta_3 & \cdots & -\delta_p \end{bmatrix}, \ \underset{p\times 1}{\hat{B}_c} = \begin{bmatrix} 0 \\ \vdots \\ 0 \\ 1 \end{bmatrix} \tag{27}$$

where the coefficients $\delta_i,\ i = 1, \ldots, p$ *are defined by the disturbance poles* $\lambda_i(\mathcal{A})$

$$\lambda^p + \delta_p \lambda^{p-1} + \cdots + \delta_1 = \prod_{i=1}^{p} (\lambda - \lambda_i) \tag{28}$$

The servo-compensator is a dynamic compensator which, by definition (28), is in resonance with the external disturbances acting on the plant. Therefore it represents an internal model of the external disturbances according to the internal model principle. Concerning the information about the disturbances, it is sufficient to know only the disturbance poles $\lambda_i(\mathcal{A})$ which characterize the disturbance type. It is not necessary to know E, F in the plant model (18, 18) nor $\mathcal{A}, \mathcal{C}$ of the disturbance model (22). The controller is robust in the sense that perfect disturbance rejection is achieved for any uncertainties in the plant model as long as the closed-loop system remains stable.

The simplest controller to achieve robust disturbance rejection consists of the servo-compensator and a static feedback gain matrix K_c, without any additional stabilizing controller. Since the servo-compensator is completely given by the knowledge of the disturbance poles (28), the only unknown parameters are contained in the static gain matrix K_c. The design problem is therefore to find the gain matrix K_c. To achieve a fast transient response, K_c is chosen to minimize a quadratic performance index according to Eqn. (12).

Stabilization

The rotor-induced vibration problem will be addressed by robust disturbance rejection control. Active damping enhancement of the weakly damped lagging motion requires additional stabilizing controllers. In the design of a decentralized stabilization, we construct a stabilizing controller from dynamic compensators of known structure. Once the structure of the compensators is determined, the remaining design problem is to find optimal parameters for the compensators. Generalized second-order filters are considered as candidates for dynamic compensators with known structure, although any other compensator may be applied, too.

For active damping enhancement, any stabilizing compensator must provide the proper gain and phase characteristics within the bandwidth of the control. The concept of generalized second-order filtering [41] allows the construction of frequency-shaped stabilizing compensators based on the classical approach of gain-phase stabilization. The generalized second-order filter is given in transfer function representation by

$$F(s) \quad = \quad k\frac{s^2/\omega_z^2 + 2\zeta_z s/\omega_z + 1}{s^2/\omega_p^2 + 2\zeta_p s/\omega_p + 1} \tag{29}$$

Depending on the choice of the coefficients $k, \zeta_z, \zeta_p, \omega_z, \omega_p$ various filters with different gain-phase characteristics can be realized from the generalized second-order filter. Based on these basic filters, a frequency-shaped stabilizing compensator can be constructed by simple series connection, e.g. a bandpass filter and a non-minimum phase allpass filter may be combined to target a certain mode and provide the proper phase characteristics. Once the structure of the stabilizing compensator is determined, the remaining parameters are then calculated within the framework of decentralized optimal output feedback.

Decentralized Vibration Control

The synthesis of a decentralized vibration control system for active helicopter rotor blades requires to set robust disturbance rejection and rotor stabilization into the framework of decentralized optimal output feedback and solve for the structured static output feedback matrix.

Let the plant to be controlled be represented by the linear time-invariant system

$$\begin{aligned}\dot{x}_p &= A_p x_p + B_p u_p + E_p w &(30)\\ y_{p_c} &= C_{p_c} x_p + D_{p_c} u_p + F_{p_c} w &(31)\\ y_{p_s} &= C_{p_s} x_p + F_{p_s} w &(32)\end{aligned}$$

where x_p denotes the state vector of the plant, u_p the input vector, w the vector of disturbances, y_{p_c} the vector of outputs to be regulated and y_{p_s} the vector of outputs amenable for stabilization. A linear time-invariant plant model representing the aeroservoelastic behavior of active helicopter rotors may be obtained by a constant coefficient approximation of the time-periodic system in multiblade coordinates.

Suppose the plant (rotor) consists of N interconnected subsystems (rotor blades) and is required to be stabilized by N individual subsystem controllers. Let the i-th subsystem controller be constructed from generalized second-order filters given by

$$\begin{aligned}\dot{\hat{x}}_{s_i} &= \hat{A}_{s_i}\hat{x}_{s_i} + \hat{B}_{s_i}\hat{u}_{s_i} &(33)\\ \hat{y}_{s_i} &= \hat{C}_{s_i}\hat{x}_{s_i} + \hat{D}_{s_i}\hat{u}_{s_i} &(34)\end{aligned}$$

Now suppose the subsystems are identical as in the case of identical rotor blades. Then there is no reason for the subsystem controllers to be non-identical, thus

$$\begin{aligned}&\hat{A}_{s_1} = \hat{A}_{s_2} = \ldots = \hat{A}_{s_N} =: \hat{A}_s &(35)\\ &\hat{B}_{s_1} = \hat{B}_{s_2} = \ldots = \hat{B}_{s_N} =: \hat{B}_s &(36)\\ &\hat{C}_{s_1} = \hat{C}_{s_2} = \ldots = \hat{C}_{s_N} =: \hat{C}_s &(37)\\ &\hat{D}_{s_1} = \hat{D}_{s_2} = \ldots = \hat{D}_{s_N} =: \hat{D}_s &(38)\end{aligned}$$

Transforming the individual subsystem controllers into multiblade coordinates, the stabilizing controller for $N = 4$ subsystems (rotor blades) is given by

$$\dot{x}_s = \underbrace{\begin{bmatrix} \hat{A}_s & 0 & 0 & 0\\ 0 & \hat{A}_s & -\Omega I & 0\\ 0 & \Omega I & \hat{A}_s & 0\\ 0 & 0 & 0 & \hat{A}_s\end{bmatrix}}_{A_s} x_s + \underbrace{\begin{bmatrix} \hat{B}_s & 0 & 0 & 0\\ 0 & \hat{B}_s & 0 & 0\\ 0 & 0 & \hat{B}_s & 0\\ 0 & 0 & 0 & \hat{B}_s\end{bmatrix}}_{B_s} u_s \quad (39)$$

$$y_s = \underbrace{\begin{bmatrix} \hat{C}_s & 0 & 0 & 0\\ 0 & \hat{C}_s & 0 & 0\\ 0 & 0 & \hat{C}_s & 0\\ 0 & 0 & 0 & \hat{C}_s\end{bmatrix}}_{C_s} x_s + \underbrace{\begin{bmatrix} \hat{D}_s & 0 & 0 & 0\\ 0 & \hat{D}_s & 0 & 0\\ 0 & 0 & \hat{D}_s & 0\\ 0 & 0 & 0 & \hat{D}_s\end{bmatrix}}_{D_s} u_s \quad (40)$$

where x_s, u_s, y_s are in multiblade coordinates. The overall decentralized vibration controller consists of compensators for robust disturbance rejection and stabilization. In order to achieve robust disturbance rejection, we apply the servo-compensator

$$\begin{aligned}\dot{x}_c &= A_c x_c + B_c y_{p_c} &(41)\\ u_{p_c} &= K_c x_c &(42)\end{aligned}$$

For stabilization, we consider the above composed stabilizing controller

$$\begin{aligned}\dot{x}_s &= A_s x_s + B_s y_{p_s} &(43)\\ u_{p_s} &= C_s x_s + D_s y_{p_s} &(44)\end{aligned}$$

Defining auxiliary inputs and outputs for the servo-compensator, i.e. $y_c := x_c$, and for the stabilizing controller, i.e. $u_s := \dot{x}_s$ and $y_s := x_s$ and applying the overall controller to the plant using $u_p = u_{p_c} + u_{p_s}$ yields the expanded system

$$\underbrace{\begin{bmatrix}\dot{x}_p\\ \dot{x}_c\\ \dot{x}_s\end{bmatrix}}_{\dot{x}} = \underbrace{\begin{bmatrix} A_p & 0 & 0\\ B_c C_{p_c} & A_c & 0\\ 0 & 0 & 0\end{bmatrix}}_{A} \underbrace{\begin{bmatrix} x_p\\ x_c\\ x_s\end{bmatrix}}_{x} + \underbrace{\begin{bmatrix} 0 & B_p\\ 0 & B_c D_{p_c}\\ I & 0\end{bmatrix}}_{B} \underbrace{\begin{bmatrix} u_s\\ u_p\end{bmatrix}}_{u} + \underbrace{\begin{bmatrix} E_p\\ B_c F_{p_c}\\ 0\end{bmatrix}}_{E} w \quad (45)$$

$$\underbrace{\begin{bmatrix} y_s\\ y_{p_s}\\ y_c\end{bmatrix}}_{y} = \underbrace{\begin{bmatrix} 0 & 0 & I\\ C_{p_s} & 0 & 0\\ 0 & I & 0\end{bmatrix}}_{C} \underbrace{\begin{bmatrix} x_p\\ x_c\\ x_s\end{bmatrix}}_{x} + \underbrace{\begin{bmatrix} 0\\ F_{p_s}\\ 0\end{bmatrix}}_{F} w \quad (46)$$

$$\underbrace{\begin{bmatrix} u_s\\ u_p\end{bmatrix}}_{u} = \underbrace{\begin{bmatrix} A_s & B_s & 0\\ C_s & D_s & K_c\end{bmatrix}}_{K} \underbrace{\begin{bmatrix} y_s\\ y_{p_s}\\ y_c\end{bmatrix}}_{y} \quad (47)$$

where all unkown parameters are contained in the static output feedback matrix K. The transient behavior in terms of the deviation from the steady-state is governed by

$$\begin{aligned}\dot{x} &= Ax + Bu &(48)\\ y &= Cx &(49)\\ u &= Ky &(50)\end{aligned}$$

where the structure of K depends on the choice of the stabilizing controller and is represented by the arbitrary feedback structure formulation given by Definition 1

$$K \;=\; K_p + \sum_{i=1}^{m} t_i\, k^T\, U_i \tag{51}$$

The controller parameters in K are then chosen in order to minimize the quadratic performance index J leading to the optimization problem for which the necessary conditions are given in Theorem 1. This unconstrained optimization problem can be solved modifying the iterative algorithm of Moerder and Calise [23] for decentralized control. The algorithm is shown to converge to a local minimum when starting from a stabilizing initial gain. Depending on the respective design specifications, constraint requirements may be imposed on decentralized optimal output feedback.

Including constraints, the optimization problem can be solved by nonlinear programming algorithms with the update of the performance index calculated from the solution of the necessary conditions of the unconstrained problem given in Theorem 1.

Design for Active Helicopter Rotor Blades

A case study for the design of decentralized vibration control systems for active helicopter rotor blades is given. Figure 4 shows the proposed control system consisting of a disturbance rejection loop for hub load compensation and $N = 4$ individual subsystem stabilizing controllers for rotor stabilization. The performance of various control design examples is investigated with a focus on robustness of the controller when applied to the correct time-periodic system. This will demonstrate the inherent robustness of the decentralized control approach.

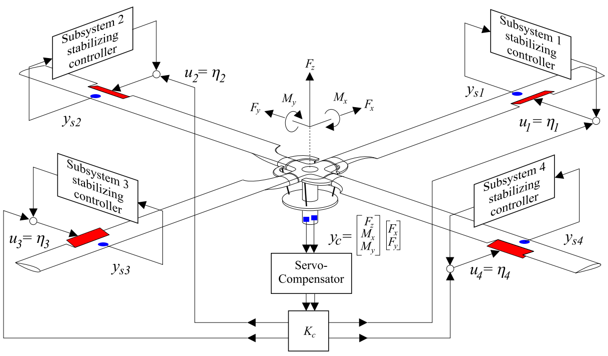

Figure 4: Decentralized rotor control system.

The control inputs are the trailing edge flap deflections η_i, $i = 1, \ldots, N$. The hub loads represent the outputs to be regulated where out-of-plane loads $y_c = [F_z, M_x, M_y]$ and in-plane loads $y_c = [F_x, F_y]$ are distinguished. The stabilizing controllers further require an additional individual rotating blade sensor signal y_{s_i}, which is assumed to be provided by a lagwise acceleration sensor on the blade. Alternatively, blade root load sensors may be applied to provide the necessary individual blade sensor signal.

Hub load Compensation

In the rotor-induced vibration problem, the control objective is the compensation of the 4Ω-hub loads. This is approached by robust disturbance rejection control RDRC. The plant is represented by the linear time-invariant system in multiblade coordinates where the input u consists of the trailing edge flap deflections in multiblade coordinates $u = [\eta_0, \eta_{1c}, \eta_{1s}, \eta_2]$ and the outputs y_c are the hub loads.

The 4Ω-hub loads generated in uncontrolled forward flight are considered as disturbances w of sinusoidal type. Applying the internal model principle to achieve robust disturbance rejection leads to the servo-compensator

$$\dot{x}_c = \underbrace{\begin{bmatrix} \begin{bmatrix} 0 & 1 \\ -(4\Omega)^2 & 0 \end{bmatrix} & 0 & 0 \\ 0 & \begin{bmatrix} 0 & 1 \\ -(4\Omega)^2 & 0 \end{bmatrix} & 0 \\ 0 & 0 & \ddots \end{bmatrix}}_{A_c} x_c + \underbrace{\begin{bmatrix} \begin{bmatrix} 0 \\ 1 \end{bmatrix} & 0 & 0 \\ 0 & \begin{bmatrix} 0 \\ 1 \end{bmatrix} & 0 \\ 0 & 0 & \ddots \end{bmatrix}}_{B_c} y_c \tag{52}$$

where the blockdiagonal matrices A_c, B_c contain exactly r identical blocks corresponding to the number of hub loads to be compensated, i.e. $r = 3$ for the out-of-plane loads $y_c = [F_z, M_x, M_y]$ and $r = 2$ for the in-plane loads $y_c = [F_x, F_y]$. Since the servo-compensator is completely given by the knowledge of the disturbance type, the remaining design problem is to find a static output feedback matrix K_c.

Decentralized optimal output feedback is applied to calculate the optimal solution subject to performance robustness with respect to tuning errors of the servo-compensator. Furthermore, the control system is required to possess robustness with respect to a variation of the flight speed regime. The control system designed for nominal high-speed flight is required to possess closed-loop stability for low speed flight as well for as hover flight encountered by a parameter uncertainty constraint.

Out-of-Plane Hub loads A typical design example for the compensation of the out-of-plane hub loads $y_c = [F_z, M_x, M_y]$ is given. The detailed parameters are summerized in Tab. 2. Figure 5(a) shows the pole map for the open-loop and closed-loop system and Fig. 5(b) the maximum singular value plot for the input disturbance transmissibility, i.e. $\overline{\sigma}(T_{wy_c})$ with $T_{wy_c} = \frac{Y_c(j\omega)}{W(j\omega)}$ where the disturbances W are applied at the input.

Table 2: Design example parameters for RDRC out-of-plane

Obj	Compensation of 4Ω out-of-plane hub loads $y_c = [F_z, M_x, M_y]$	
Plant	BO105, 114 KTAS, TEF at 65% radius, hub load sensors	
Control	Robust disturbance rejection controller consisting of • servo-compensator given by Eqn. (52) • static output feedback matrix K_c	
Weight	$Q = I \quad R = 10^{-5} I$	
Constr. req.	Pole region	Performance robustness
	$\underline{\zeta} = 0.25\%$ $\underline{\delta} = 0.018$ 1/rev	T : 20dB below uncontr. $N = 1.3\%$

The effect of robust disturbance rejection control in the closed-loop is the following: The 3-fold poles of the servo-compensator separate from their open-loop values $\lambda = \pm j4\Omega$. As a result, shown in the singular value plot, the disturbance transmissibility becomes zero at 4Ω – a transmission zero has been introduced. This provides the required compensation of the 4Ω-hub loads since for any disturbances acting on the system, no outputs will be observed in the steady-state at frequency 4Ω.

The time response of the closed-loop system is shown in Fig. 6. The response is given for the controller applied to the time-invariant LTI system, i.e. the plant model used for controller design, as well as the correct time-periodic LTP system.

The transient behavior of the regulated and unregulated hub loads due to persistent 4Ω disturbances is plotted as the control loop is closed. The regulated hub loads decay rapidly with the unregulated hub loads remaining almost unchanged. Trailing edge flap deflections of about $2.5°$ are required to compensate the out-of-plane hub loads. For the time-periodic system, it turns out that perfect disturbance rejection is still achieved for the 4Ω disturbances. However, comparing the regulated hub loads for the time-invariant and the time-periodic system, it is observed that the action of the controller applied to the time-periodic system generates static as well as 8Ω-hub loads.

<u>In-Plane hub loads</u> The compensation of in-plane hub loads $y_c = [F_x, F_y]$ is different from the out-of-plane case since in-plane hub loads are due to the in-plane lagging motion which is weakly damped. This will make the application of robust disturbance rejection control without lagging mode stabilization insufficient in the in-plane case.

Figure 7 shows the time response of the open-loop and closed-loop system. In Fig. 7(a), the transient response of the regulated hub loads is shown as the control loop is closed whereas in Fig. 7(b) the impulse response for a differential input disturbance is given. The impulse response represents the situation of the control system

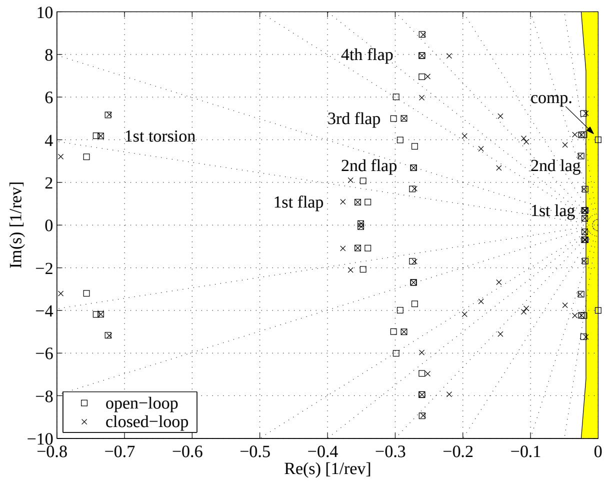

(a) Pole map

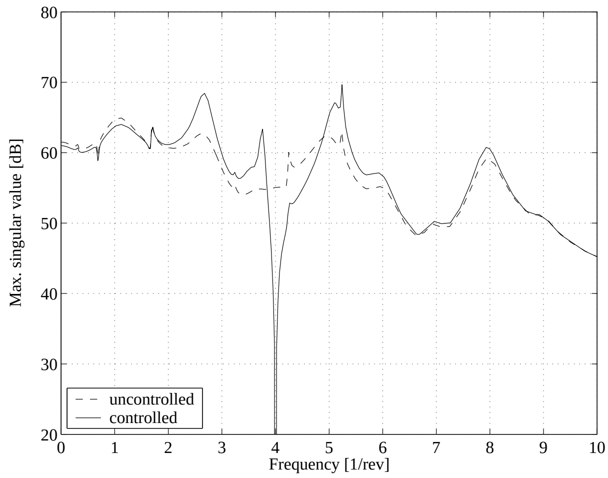

(b) Disturbance transmissibility

Figure 5: Pole map and disturbance transmissibility for RDRC out-of-plane.

in unsteady flight conditions, e.g. when the rotor blades are affected by gust loads.

Whereas the transient response decays sufficiently fast after the control loop is closed, the speed of the impulse response is quite insufficient. Depending on the frequency of occurance of gust loads, the rotor may hardly remain in steady-state where the hub filtering characteristics apply and the transmitted 4Ω-hub loads are compensated by the controller. In unsteady flight, the motion of the rotor blades is not periodic and all frequencies are transmitted through the hub. However, the servo-compensator provides hub load compensation near 4Ω only. Therefore, compensation of in-plane hub loads without additional lagging mode stabilization is not very effective.

<u>Rotor Stabilization</u>

In the rotor stabilization problem, the control objective is the active damping enhancement of the aerodynamically weakly damped lagging motion. The plant is again represented by the linear time-invariant system in multiblade coordinates. Input u and output y_s consist

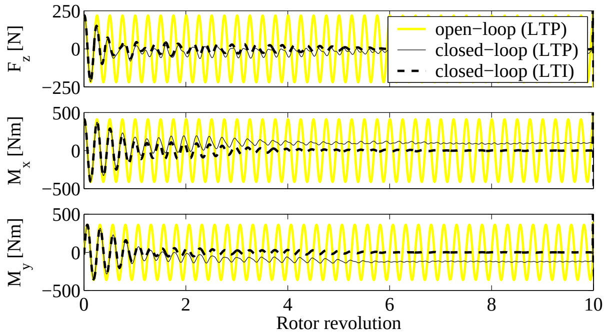

(a) Regulated hub loads

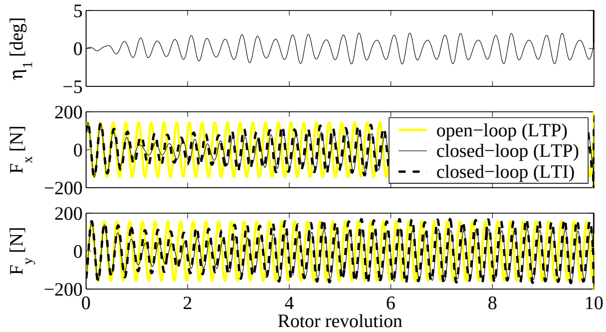

(b) TEF deflection and unregulated hub loads

Figure 6: Time response for RDRC out-of-plane.

of individual rotating blade actuator and sensor signals both transformed into multiblade coordinates.

Considering the rotor as an interconnection of N subsystems (rotor blades), we require the stabilizing controller to consist of N identical subsystem stabilizing controllers as described. The individual subsystem stabilizing controllers are constructed from the generalized second-order filter given by Eqn. (29). A fixed bandpass filter

$$F_{bp}(s) = \frac{2\zeta_{bp}s/\omega_{bp}}{s^2/\omega_{bp}^2 + 2\zeta_{bp}s/\omega_{bp} + 1} \tag{53}$$

with parameters ζ_{bp}, ω_{bp} is chosen to target the 2nd lagging mode and to provide -20dB/decade roll-off for gain stabilization of the higher (unmodeled) modes. In addition, two non-minimum phase allpass filters

$$F_i(s) = \sqrt{g}\,\frac{s^2/\omega_i^2 - 2\zeta_i s/\omega_i + 1}{s^2/\omega_i^2 + 2\zeta_i s/\omega_i + 1}, i = 1,2 \tag{54}$$

are applied with parameters $\zeta_i, \omega_i, g,\ i = 1,2$ being determined to provide the proper phase characteristics for phase stabilization of the 1st and 2nd lagging mode. The two non-minimum phase allpass filters, connected in series, build the identical subsystem stabilizing controllers given by

Table 3: Design example parameters for RDRC in-plane

Obj	Compensation of 4Ω in-plane hub loads $y_c = [F_x, F_y]$	
Plant	BO105, 114 KTAS, TEF at 65% radius, hub load sensors	
Control	Robust disturbance rejection controller consisting of • servo-compensator given by Eqn. 52 • static output feedback matrix K_c	
Weight	$Q = H^T H$ with $x_c = Hx$ $\quad R = 10^{-5} I$	
Constr. req.	Pole region	Performance robustness
	$\underline{\zeta} = 0.25\%$	T : 15dB below uncontr.
	$\underline{\delta} = 0.009$ 1/rev	$N = 1.2\%$

$$\dot{\hat{x}}_s = \underbrace{\begin{bmatrix} 0 & 1 & 0 & 0 \\ -\omega_1^2 & -2\zeta_1\omega_1 & 0 & 0 \\ 0 & 0 & 0 & 1 \\ 0 & -4\zeta_1\omega_1 & -\omega_2^2 & -2\zeta_2\omega_2 \end{bmatrix}}_{\hat{A}_s} \hat{x}_s + \underbrace{\begin{bmatrix} 0 \\ g \\ 0 \\ g \end{bmatrix}}_{\hat{B}_s} \hat{u}_s \tag{55}$$

$$\hat{y}_s = \underbrace{\begin{bmatrix} 0 & -4\zeta_1\omega_1 & 0 & -4\zeta_2\omega_2 \end{bmatrix}}_{\hat{C}_s} \hat{x}_s + \underbrace{\begin{bmatrix} g \end{bmatrix}}_{\hat{D}_s} \hat{u}_s \tag{56}$$

Transformation of the N individual subsystem stabilizing controllers into multiblade coordinates following Eqs. (39, 40) yields the stabilizing controller. Defining an expanded system similar to Eqs. (45, 46, 47) leads to a static output feedback problem where we have to determine the structured static output feedback matrix $K = K_p + \sum_{i=1}^{m} t_i\, k^T\, U_i$ written as

$$K = \left[\begin{array}{cccc|cccc} \hat{A}_s & 0 & 0 & 0 & \hat{B}_s & 0 & 0 & 0 \\ 0 & \hat{A}_s & -\Omega I & 0 & 0 & \hat{B}_s & 0 & 0 \\ 0 & \Omega I & \hat{A}_s & 0 & 0 & 0 & \hat{B}_s & 0 \\ 0 & 0 & 0 & \hat{A}_s & 0 & 0 & 0 & \hat{B}_s \\ \hline \hat{C}_s & 0 & 0 & 0 & \hat{D}_s & 0 & 0 & 0 \\ 0 & \hat{C}_s & 0 & 0 & 0 & \hat{D}_s & 0 & 0 \\ 0 & 0 & \hat{C}_s & 0 & 0 & 0 & \hat{D}_s & 0 \\ 0 & 0 & 0 & \hat{C}_s & 0 & 0 & 0 & \hat{D}_s \end{array}\right] \tag{57}$$

The parameters to be designed are contained in the vector k

$$k^T = \begin{bmatrix} -\omega_1^2 & -2\zeta_1\omega_1 & -\omega_2^2 & -2\zeta_2\omega_2 & g \end{bmatrix} \tag{58}$$

Once k is determined, the parameters $\zeta_1, \omega_1, \zeta_2, \omega_2, g$ of the non-minimum phase allpass filters can be recovered uniquely provided the signs of the elements in k are correct. Decentralized optimal output feedback subject to inequality constraints is applied to calculate the optimal solution, see Tab. 4.

The damping ratio is increased from $1-5\%$ to $6-20\%$ for the 1st and from $0.5-1\%$ to $3-6\%$ for the 2nd lagging mode. The behavior of the decentralized stabilizing controller applied to the time-periodic system

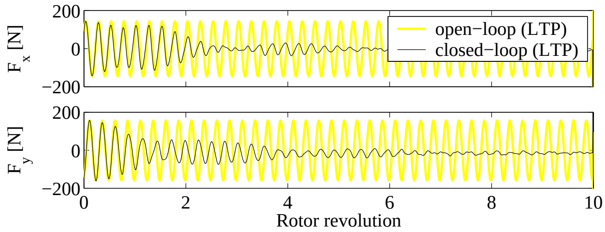

(a) Transient response

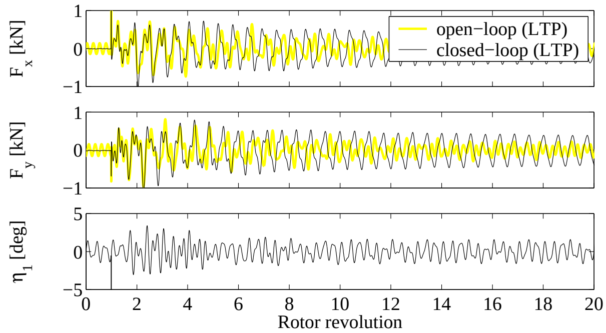

(b) Impulse response (differential)

Figure 7: Time response for RDRC in-plane.

Table 4: Design example parameters for LMS

Obj	Damping of 1st and 2nd lagging mode				
Plant	BO105, 114 KTAS, TEF at 65% and lagwise displacement sensors at 55% radius				
Control	N identical subsystem stabilizing controllers consisting of • fixed bandpass with $\zeta_{bp} = 0.2$, $\omega_{bp} = 4.23$/rev • two non-minimum phase allpass filters				
Weight	$Q = I \quad R = 10^{-5} I$				
Constr. req.	Pole region $\underline{\zeta} = .03, \underline{\delta} = .07$/rev		Controller param. $\zeta_i \geq .3,\ \omega_i > 0$		
Param.	ζ_1	ω_1	ζ_2	ω_2	$-g$
initial	0.36	1.0/rev	2.2	5.8/rev	10^3
optimal	0.92	2.0/rev	1.2	2.5/rev	10^4
Damping	1st lag		2nd lag		
uncontr.	$1-5\%$		$0.5-1\%$		
contr.	$6-20\%$		$3-6\%$		
Increase	400%		600%		

can be seen from the impulse response. Figure 8 shows the lagwise displacement outputs in collective y_{ζ_0}, cyclic $y_{\zeta_{1c}}, y_{\zeta_{1s}}$ and differential y_{ζ_2} form due to an impulse disturbance applied to the differential input. The response involving the correct time-periodic LTP system is compared to the response involving the approximate time-invariant LTI design model. The damping enhancement achieved with the LTI design model is actually realized for the LTP system, thus justifying controller design based on LTI systems.

The inherent robustness of decentralized control with respect to the interconnection error becomes evident, too. The open-loop response of the LTP system is matched by the LTI system solely in the differential output y_{ζ_2}, whereas the interconnection with all non-differential outputs $y_{\zeta_0}, y_{\zeta_{1c}}, y_{\zeta_{1s}}$ is not included in the LTI design model. However, the decentralized stabilizing controller applied to the time-periodic system provides excellent performance, see Fig. 8(b). The non-differential outputs $y_{\zeta_0}, y_{\zeta_{1c}}, y_{\zeta_{1s}}$ decay as fast as the differential output y_{ζ_2}, although the interconnection was not included in the LTI design model. This clearly demonstrates the inherent robustness of the decentralized control approach with respect to uncertain subsystem interconnections.

Hub Load Compensation and Rotor Stabilization

Finally, hub load compensation by robust disturbance rejection control is applied with rotor stabilization by N identical subsystem stabilizing controllers. This yields the complete decentralized vibration control system.

The control objective in this case is to compensate the 4Ω in-plane hub loads while providing lagging mode stabilization in order to reach the steady-state sufficiently fast as the rotor blades are affected by gust loads. In Fig. 9, three design examples with different performance robustness requirements are compared, see Tab. 5.

As a result of the non-collocated system behavior, a decrease in damping is associated with robust disturbance rejection control. The higher the required performance robustness, the lower the achievable active damping enhancement. The design example B represents a balanced design which achieves moderate performance robustness with sufficient damping enhancement. The input disturbance transmissibility is ensured to stay 15 dB below the uncontrolled level within a 1% frequency band while damping enhancement of about 400% for the 1st and 500% for the 2nd lagging mode is achieved.

The enhancement of the time response is shown in Fig. 10. The speed of the impulse response, again shown for a differential input disturbance, is increased substantially compared to the case without lagging mode stabilization. Thus, when the rotor blades are exposed to gust loads, the rotor reaches rapidly the steady-state where the 4Ω-hub loads are compensated. The trailing edge flap deflections for hub load compensation with lagging mode stabilization are comparable to the case of hub load compensation only.

Similarly, a compensation of out-of-plane hub loads can be achieved with simultaneous lagging mode or flapping mode stabilization, for details see [19].

Conclusions and Perspective

The objective of this research has been to develop a vibration control method for active helicopter rotor blades in order to achieve simultaneously rotor-induced vibration reduction and rotor stabilization.

The time-periodic behavior of the individual rotor blades has been approximated by a time-invariant system

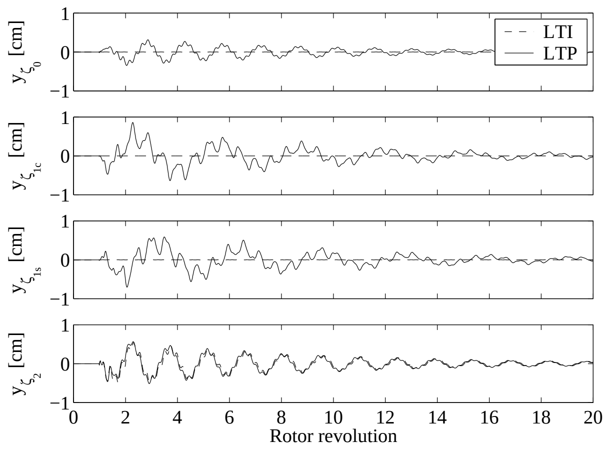

(a) Open-loop system

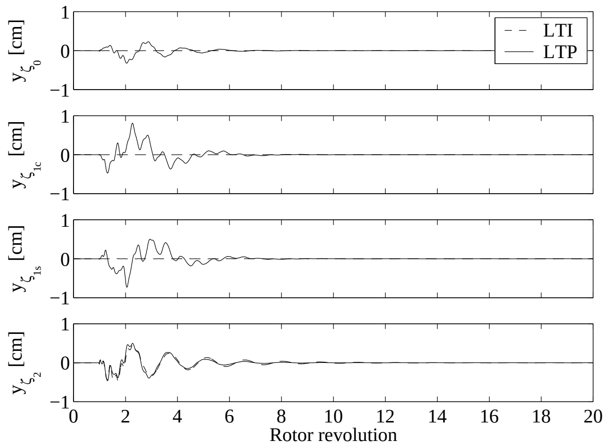

(b) Closed-loop system

Figure 8: Impulse response due to a differential input disturbance for LMS.

representing the rotor as a whole. Considering the rotor as an interconnection of N subsystems (rotor blades), the approximation has been investigated in terms of subsystem interconnection errors.

A new vibration control method has been proposed based on decentralized control which provides inherent robustness with respect to uncertain subsystem interconnections and is therefore appropriate to control the time-periodic behavior of active helicopter rotor blades. The internal model principle has been applied to achieve hub load compensation by robust disturbance rejection. Rotor stabilization has been addressed by subsystem stabilizing controllers constructed from dynamic compensators of known structure. The synthesis of the decentralized vibration control system is finally done introducing the framework of decentralized optimal output feedback.

The application to active helicopter rotor blades clearly demonstrates that the time-periodic behavior of a rotor in forward flight could be controlled by time-invariant controllers. Furthermore, the design of such time-invariant controllers can be performed based on a time-invariant approximation of the plant model. Although a considerable error, called the subsystem interconnection error, is introduced by the approximation, the inherent robustness of the proposed decentralized control approach allows controller design based on time-invariant systems. This introduces a considerable simplification into the control system and degrades the periodic control concepts proposed for vibration reduction and rotor stabilization in the past. The control system is robust with respect to a variation of the flight speed regime and reliable with respect to the failure of a single subsystem stabilizing controller. Active damping enhancement of about 500% is achieved for the 1st and 2nd in-plane lagging modes while a maximum out-of-plane hub load reduction of 20 dB within a 5% frequency band can be obtained.

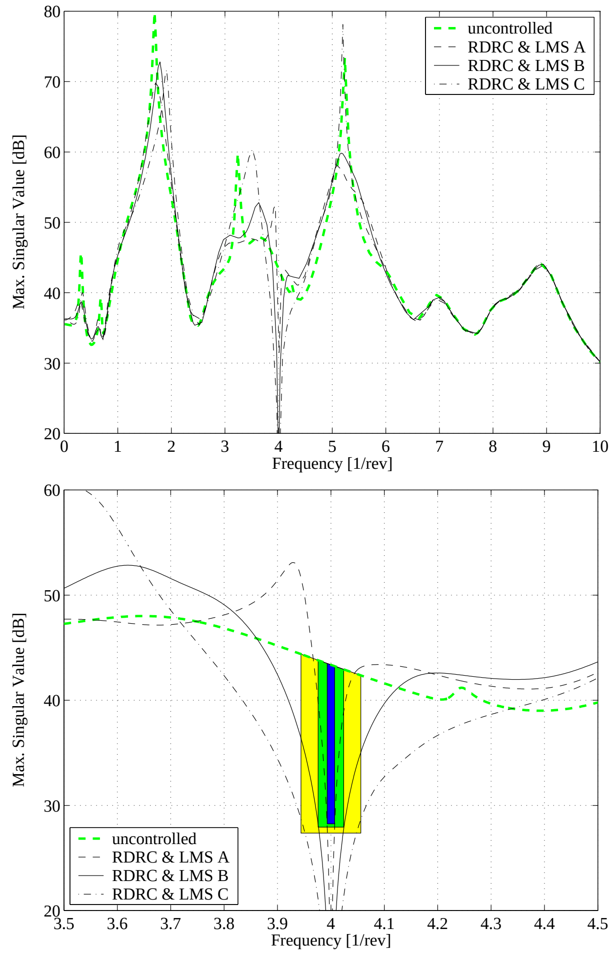

Figure 9: Disturbance transmissibility for RDRC & LMS in-plane.

The decentralized control approach is however based on the availability of individual subsystem (rotating blade) sensors which may not be required by standard centralized control. The conceptually simple feedback structure and the inherent robustness of decentralized control has been achieved at the expense of additional rotating blade sensors.

References

[1] P. Arcara, S. Bittanti, and M. Lovera. Periodic control of helicopter rotors for attenuation of vibrations

Table 5: Design example parameters for RDRC & LMS B

Obj	Compensation of 4Ω in-plane hub loads $y_c = [F_x, F_y]$ and damping of 1st and 2nd lagging mode				
Plant	BO105, 114 KTAS, TEF at 65% and lagwise displacement sensors at 55% radius, hub load sensors				
Control	Robust disturbance rejection controller consisting of • servo-compensator given by Eqn. (52) • static output feedback matrix K_c and N identical subsystem stabilizing controllers consisting of • fixed bandpass with $\zeta_{bp} = 0.2$, $\omega_{bp} = 4.23$/rev • two non-minimum phase allpass filters				
Weight	$Q = H^T H$ with $x_c = Hx \quad R = 10^{-5} I$				
Constr.	Pole region		Controller param.		
req.	$\underline{\zeta} = .025,\ \underline{\delta} = .06$/rev		$\zeta_i \geq 0.3,\ \omega_i > 0$		
	Performance robustness				
	$\overline{T}$: 15dB below uncontr.				
	$N_B = 1\%\quad N_A = 0.35\%\quad N_C = 2.6\%$				
Param.	ζ_1	ω_1	ζ_2	ω_2	$-g$
optimal	0.9	2/rev	0.9	2/rev	10^4
Damping	1st lag		2nd lag		
uncontr.	$1-5\%$		$0.5-1\%$		
contr.	$4-20\%$		$2.5-10\%$		
Increase	400%		500%		

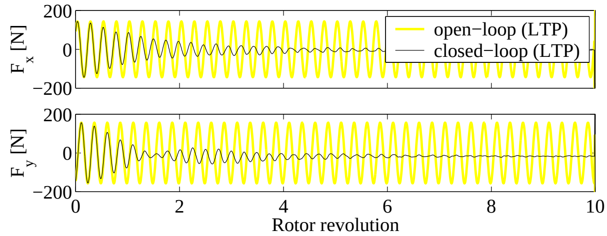

(a) Transient response

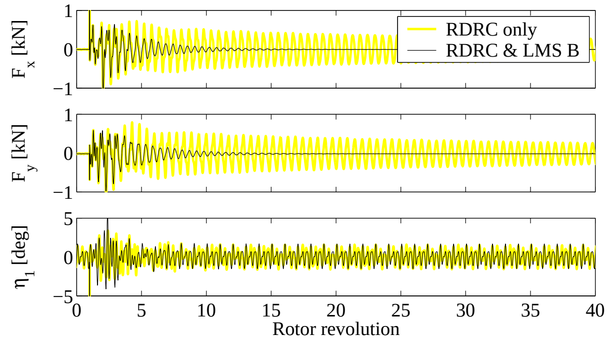

(b) Impulse response (differential)

Figure 10: Time response for RDRC & LMS in-plane.

in forward flight. *IEEE Transactions on Control System Technology*, 8(6):883 – 894, 2000.

[2] R. Barrett. Design, construction and characterization of a flightworthy piezoelectric solid state adaptive rotor. *Smart Materials and Structures*, 7(3):422 – 431, 1998.

[3] A. Büter. *Untersuchung adaptiver Konzepte zur Reduktion von Hubschraubervibrationen, zur Minderung des Hubschrauberlärms und zur Steigerung der aerodynamischen Effizienz*. PhD thesis, Institut für Strukturmechanik, DLR, 1998.

[4] R. A. Calico and W. E. Wiesel. Stabilization of helicopter blade flapping. *Journal of the American Helicopter Society*, 31(4):59 – 64, 1986.

[5] A. J. Calise, M. E. Wasikowski, and D. P. Schrage. Optimal output feedback for linear time-periodic systems. *Journal of Guidance, Control, and Dynamics*, 15(2):416 – 423, 1992.

[6] P. C. Chen and I. Chopra. Hover testing of smart rotor with induced-strain actuation of blade twist. *AIAA Journal*, 35, 1997.

[7] I. Chopra. Status of application of smart structures technology to rotorcraft systems. *Journal of the American Helicopter Society*, 45(4), 2000.

[8] R. P. Coleman. Theory of self-excited mechanical oscillations of hinged rotor blades. Technical report, NACA, 1943.

[9] E. J. Davison. *The Control Handbook*, chapter Robust Servomechanism Problem, pages 731 – 747. CRC Press, 1996.

[10] R. C. Derhman and N. W. Hagood. Rotor design using smart materials to actively twist blades. In *American Helicopter Society 52nd Annual Forum*, pages 1242 – 1252, 1996.

[11] O. Dieterich. Application of modern control technology for advanced IBC systems. In *24th European Rotorcraft Forum*, page AS03, 1998.

[12] B. Enenkl, V. Klöppel, D. Preiler, and P. Jänker. Full-scale rotor with piezoelectric actuated blade flaps. In *28th European Rotorcraft Forum*, 2002.

[13] O. Föllinger. *Optimierung dynamischer Systeme*. Oldenbourg, 1988.

[14] S. R. Hall and E. F. Prechtl. Preliminary testing of a mach-scaled active rotor blade with a trailing-edge servo flap. In *SPIE Proceedings of Smart Structures and Materials 1999*, volume 3668, pages 14 – 21, 1999.

[15] S. R. Hall and N. M. Wereley. Performance of higher harmonic control algorithms for helicopter vibration

reduction. *Journal of Guidance, Control and Dynamics*, 16(4):793 – 797, 1992.

[16] N. D. Ham. Helicopter individual-blade-control research at MIT 1977 – 1985. *Vertica*, 11(1/2):109 – 122, 1987.

[17] W. Johnson. *A Comprehensive Analytical Model of Rotorcraft Aerodynamics and Dynamics – Theory Manual*. Johnson Aeronautics, 1996.

[18] C. Kessler and G. Reichert. Active control to augment rotor lead-lag damping. *The Aeronautical Journal*, pages 245 – 258, 1998.

[19] P. Konstanzer. *Decentralized Vibration Control for Active Helicopter Rotor Blades*. PhD thesis, Institute of Statics and Dynamics of Aerospace Structures, University of Stuttgart, VDI Fortschritt-Berichte, 8(923), 2002.

[20] N. A. Koratkar and I. Chopra. Hover testing of a mach-scaled rotor with piezoelectric-bender-actuated trailing edge flaps. In *SPIE Proceedings of Smart Structures and Materials 2000*, volume 3985, pages 2 – 10, 2000.

[21] F. L. Lewis and V. L. Syrmos. *Optimal Control*. John Wiley & Sons, 1995.

[22] J. Milgram and I. Chopra. Dynamically tuned blade pitch links for vibration reduction. In *American Helicopter Society 50th Annual Forum*, 1994.

[23] D. D. Moerder and A. J. Calise. Convergence of a numerical algorithm for calculating optimal output feedback gains. *IEEE Transactions on Automatic Control*, 30(9):900 – 903, 1985.

[24] J. P. Narkiewicz. Effectiveness of time domain control algorithm for influencing rotor blade motion via trailing edge tab. In *24th European Rotorcraft Forum*, page DY16.1, 1999.

[25] C. Nett, D. Bernstein, and W. Haddad. Minimal complexity control law synthesis. Part I: Problem formulation and reduction to optimal static output feedback. In *Proceeding of the American Control Conference*, pages 2056 – 2064, 1989.

[26] F. Nitzsche. A new individual blade control approach to attenuate rotor vibration. In *22th European Rotorcraft Forum*, pages 8.1 – 8.9, 1996.

[27] R. Pandiyan and S. C. Sinha. Periodic flap control of a helicopter blade in forward flight. *Journal of Vibration and Control*, 5:761 – 777, 1999.

[28] E. F. Prechtl and S. R. Hall. An X-frame actuator servo-flap actuation system for rotor control. *SPIE Proceedings of Smart Structures and Materials 1998: Smart Structures and Integrated Systems*, 3329, 1998.

[29] E. F. Prechtl and S. R. Hall. Design of a high efficiency, large stroke, electromechanical actuator. *Smart Materials and Structures*, 18:13 – 30, 1999.

[30] E. F. Prechtl and S. R. Hall. Closed-loop vibration control experiments on a rotor with blade mounted actuation. In *41st AIAA/ASME/ASCE/AHS/ASC Structures, Structural Dynamics and Materials Conference*, pages A00–24624, 2000.

[31] J. P. Rogers and N. W. Hagood. Preliminary mach-scaled hover testing of an integral twist-actuated rotor blade. In *SPIE Proceedings of Smart Structures and Materials 1998*, 1998.

[32] H. Rottmayr, W. Popp, and R. Mehlhose. Application of modern vibration control techniques on EC135 and future trends. In *23rd European Rotorcraft Forum*, pages 51.1 – 51.17, 1997.

[33] D. K. Samak and I. Chopra. Design of high force, high displacement actuators for helicopter rotors. *Smart Materials and Structures*, 5, 1996.

[34] D. Schimke, P. Jänker, V. Wendt, and B. Junker. Wind tunnel evaluation of a full scale piezoelectric flap control unit. In *24th European Rotorcraft Forum*, page TE02, 1998.

[35] J. Shaw, N. Albion, E. J. Hanker, and R. S. Teal. Higher harmonic control: Wind tunnel demonstration of fully effective vibratory hub force suppression. *Journal of the American Helicopter Society*, 34(1):14 – 25, 1989.

[36] D. D. Siljak. *Decentralized Control of Complex Systems*. Academic Press, 1991.

[37] R. L. Spangler and S. R. Hall. Piezoelectric actuators for helicopter rotor control. In *31th AIAA/ASME/ASCE/AHS/ASC Structures, Structural Dynamics and Materials Conference*, 1990.

[38] M. G. Spencer, R. M. Sanner, and I. Chopra. Closed-loop hover test results with a neurocontroller on piezoactuated smart rotor blades. In *SPIE Proceedings of Smart Structures and Materials 2000*, volume 3985, pages 52 – 61, 2000.

[39] F. K. Straub and D. J. Merkley. Design of a smart material actuator for rotor control. *Smart Materials and Structures*, 5:68 – 75, 1996.

[40] F. K. Straub and D. J. Merkley. Design of a servo-flap rotor for reduced control loads. *Smart Materials and Structures*, 16:223 – 234, 1997.

[41] B. Wie and K.-W. Byun. New generalized structural filtering concept for active vibration control synthesis. *Journal of Guidance, Control, and Dynamics*, 12:147 – 154, 1989.